

ARTICLES

Geometrical Parameters Controlling Sensitivity of Nanoshell Plasmon Resonances to Changes in Dielectric Environment

Felicia Tam,[†] Cristin Moran,[‡] and Naomi Halas^{*,‡,§}*Department of Physics and Astronomy, Department of Chemistry, and Department of Electrical and Computer Engineering, Rice University, Houston, Texas 77005**Received: April 6, 2004; In Final Form: June 11, 2004*

In this study, we investigate the geometrical parameters that control the sensitivity of the plasmon resonance wavelength of a silica–gold nanoshell to changes in its dielectric environment. It was found that the magnitude of the SPR frequency shift upon a change in refractive index of the embedding medium depends primarily on total nanoparticle size and less sensitively on the core/shell ratio. Immobilized nanoshells on a glass substrate showed a 25% decrease in magnitude of the SPR shifts; however, sensitivities as large as $\Delta\lambda/\Delta n = 555.4$ nm/RIU were obtained for this geometry.

Introduction

There is a great deal of current interest in the optical resonant properties of metal nanoparticles. Plasmons, the collective oscillation of conduction electrons in metals, give rise to the strong optical resonances of metallic nanostructures. The plasmon resonant frequency is determined by the dielectric properties of the metal, and specifically for nanoscale metallic structures, by the size,¹ shape,² and local environment^{3–5} of the nanostructure. These plasmonic properties are being widely exploited in various current and potential technological applications, ranging from chemical sensing of various modalities,^{4,6–10} to subwavelength optical waveguides,^{11–13} to cancer detection and therapy.^{14,15}

Plasmon-resonance-based chemical sensing can be accomplished in a variety of ways. Historically, surface plasmon (SP) propagation on functionalized continuous metal films was exploited.^{16,17} Modifications in the chemical environment due to binding of molecules to the functionalized film can be monitored as changes in the angle of incidence required for surface plasmon excitation in an evanescent coupling geometry.¹⁸ More recently, localized metal nanostructures and nanopatterned surfaces have also been used as nanoscale SPR sensors, both in solution and immobilized on surfaces.^{4,19,20} In surface plasmon resonance (SPR) spectroscopy, the wavelength shift of the plasmon resonance is monitored as the refractive index of the medium surrounding the metal is changed. Nanoparticle-based SPR sensors are typically realized using direct optical transmission or reflection, since plasmon excitation on subwavelength structures does not require evanescent wave excitation.²¹ In these cases, changes in the plasmon resonance energy due to modifications in the refractive index of the surrounding medium are detected as wavelength shifts of the

plasmon resonance spectrum for dispersed nanoparticles or nanoparticles on a substrate. SPR sensing of this type can also be amplified by the use of other, functionalized nanoparticles. In these cases, the optical response of binding receptor molecules to an analyte target molecule can be engineered to induce nanoparticle aggregation, resulting in dramatic change in the optical signal due to the interparticle, or aggregate, plasmon response.^{7,22} The plasmon-induced enhancement of the electromagnetic field near the metal surface can also be used to amplify the signals of such spectroscopies as fluorescence and Raman scattering.^{6,9,23–25}

In this work, we examine the sensitivity of the plasmon response of nanoshells to changes in their dielectric environment, to investigate their efficacy as SPR nanosensors. Nanoshells are metalodielectric core–shell nanoparticles consisting of a dielectric core and a metal shell.²⁶ Nanoparticles with this geometry possess a tunable plasmon resonance that is a sensitive function of their relative core and shell dimensions.²⁷ The tunable nanoshell plasmon is a hybrid plasmon response based on an interaction between the surface plasmons supported by the inner and outer surfaces of the metallic shell layer.²⁸ Recent studies have also shown that the optically excitable plasmon of the nanoshell geometry is particularly sensitive to changes in its local dielectric environment.²⁹ Varying the absolute size of the core and shell layers introduces additional variables into the plasmon response of the nanoshell. As the overall size of the nanostructure is increased from the quasistatic limit, the optical extinction changes from primarily absorbing to primarily scattering.³⁰ With increasing nanoparticle size, additional multipolar modes are optically excited in the nanostructure. These spectrally distinct multipolar modes each have a different relative contribution of absorption and scattering to the overall plasmonic response of the nanostructure.³¹

In this series of experiments, nanoshells fabricated with a SiO₂ core and a Au shell were used to determine the effect of the dimensions of the core and shell on the SPR sensitivity. Nanoshells were immersed in media of varying refractive index

^{*} halas@rice.edu.[†] Department of Physics and Astronomy, Rice University.[‡] Department of Chemistry, Rice University.[§] Department of Electrical and Computer Engineering, Rice University.

and the wavelength of the peak plasmon wavelength was monitored. SPR sensitivity was determined by comparing the plasmon peak wavelength shift to the change in the refractive index of the surrounding medium. The core/shell ratio, absolute nanoparticle size, and the relative SPR sensitivity of the dipole vs quadrupole plasmon mode were studied, both experimentally and theoretically. Two sampling geometries were investigated: isolated nanoshells in solutions of various refractive indices and dilute nanoshells randomly deposited onto transparent dielectric substrates.³² Our studies confirm that it is indeed possible to develop highly sensitive SPR-based sensors using nanoshells both in solution and immobilized on a dielectric surface.

Experimental Section

Tetraethyl orthosilicate (TEOS, 99.9999%), (3-aminopropyl) triethoxysilane (APTES), tetrachloroauric acid, *n*-dodecanethiol, and poly(4-vinylpyridine) (160 000 MW) were obtained from Sigma-Aldrich (St. Louis, MO). TEOS was further distilled before use and all other chemicals were used as received. Ammonium hydroxide, ethanol, hexane, toluene, carbon disulfide, and chloroform were obtained from Fisher Scientific (Hampton, NH). Ultrapure water (18.2 M Ω resistivity) was obtained from a Milli-Q water purification system (Millipore, Billerica, MA). Glass microscope slides were obtained from Gold Seal Products (Portsmouth, NH). Spectral measurements were made using a Varian Cary 5000 UV-vis-NIR spectrophotometer. Particle sizes were measured using a JEOL 6500 scanning electron microscope.

Gold nanoshells were fabricated as described previously.²⁶ Briefly, monodisperse silica nanoparticles were synthesized by the hydrolysis of TEOS in basic solution via the Stöber method and functionalized with APTES in ethanol overnight. These functionalized particles are decorated with a small gold colloid (2–3 nm) prepared by the method of Duff et al.³³ A continuous gold shell is grown by reducing gold from a 1% solution of HAuCl₄ onto the attached small colloid in the presence of formaldehyde.

Some nanoshells were functionalized with dodecanethiol to facilitate transfer in solution into certain organic solvents without aggregation. The nanoshells were dispersed in a 14 mM dodecanethiol solution in ethanol and allowed to incubate for 8 h. The excess thiol was removed from the functionalized nanoshells by centrifugation. Transfer of the thiolated nanoshells into different solvents was also achieved through two cycles of centrifugation and redispersion.

Nanoshell films were prepared by immobilization of the particles on glass substrates functionalized with poly(vinylpyridine) (PVP) (MW 160 000).³² Briefly, glass slides were cleaned in piranha solution (sulfuric acid/hydrogen peroxide, 7:3) and immersed in a 1 wt % solution of PVP in ethanol. *Caution! Piranha solution is a very strong oxidizing agent and reacts violently with organic compounds. It should be handled with extreme care.* After 12 h, the slides were rinsed thoroughly with ethanol and dried with N₂. The PVP-functionalized substrates were immersed in an aqueous solution of nanoshells without thiol modification for 1 h. Upon removal from the nanoshell solution, the films were rinsed with ethanol and dried with N₂. This resulted in a submonolayer of individual nanoshells immobilized on the PVP functionalized surface. Spectral measurements were performed by inserting the nanoshell films into quartz cuvettes filled with different solvents and measuring the extinction at normal incidence. Between each solvent measurement, the films were rinsed with ethanol and dried with N₂, and the UV-vis-NIR spectrum was measured

in air to ensure that the solvents were not causing the nanoshells to detach from the surface or to aggregate.

Results and Discussion

To investigate the geometric factors affecting the sensitivity of a nanoshell SPR sensor, Mie scattering theory³⁴ was used to calculate the extinction cross-sections of nanoshells with varying dimensions. Both the overall particle size and the relative dimensions of the silica core radius (r_1) and the total particle radius (r_2) were varied. Theoretical extinction spectra were calculated for nanoshells surrounded by a homogeneous dielectric environment of refractive index n_1 (Figure 1). As n_1 is increased from 1.22 to 1.64 (Figure 1a), two distinct trends are observed: both the dipole and quadrupole plasmon resonances red shift, and the relative strength of the quadrupole resonance increases with respect to the dipole resonance. The plasmon red shifts are consistent with the increased polarizability of the dielectric media, decreasing the restoring force for the electron oscillation in the metal, thereby damping the plasmon oscillations.²⁹ The strengthening of the quadrupole resonance is a result of phase retardation effects caused by the reduced wavelength of light in a dielectric medium. As incident radiation passes through a dielectric medium, the wavelength of light is reduced. As a result, the apparent size of the nanoshell increases with respect to the wavelength of light, which results in an increase in the strength of the quadrupole excitation.³¹

From the calculated spectra, the dipole resonance shift is measured as a function of the surrounding medium's refractive index for nanoshells with constant r_1/r_2 and increasing overall size (Figure 1b). The SPR sensitivity of a nanoshell is determined by comparing the change in peak dipole wavelength for a corresponding change in solvent refractive index ($\Delta\lambda/\Delta n$) as measured in nm/refractive index unit (RIU). As the nanoshells increase in size from $r_2 = 50$ to 175 nm, the SPR sensitivity increases from 570.3 to 995.6 nm/RIU. Previous studies have investigated the effects of changing certain dimensions of nanoparticles for use as SPR sensors.³⁵ However, the change of one dimension constitutes a change in nanoparticle shape. Numerous studies have shown that SPR sensitivity is highly dependent upon the shape of the nanoparticle used.^{36,37} With the concentric sphere geometry of nanoshells, it is possible to isolate the effects of changing nanoparticle size from those of varying nanoparticle shape. To the best of our knowledge, the effect of isotropically increasing nanoparticle size on SPR sensitivity has not been previously investigated.

Recent studies report that a hollow sphere is more sensitive to local dielectric changes than a solid sphere of the same size.³⁷ Sun and Xia found that for particles with a diameter of 50 nm, the SPR sensitivity of the nanoshells with a shell thickness of 4.5 nm compared to that of solid gold colloid is almost 600% greater.³⁷ The nanoshells in their system are hollow, and the core is believed to be filled with the surrounding solvent. To investigate the effect of shell thickness on the SPR sensitivity of a nanoshell having a constant core dielectric, the extinction spectra are calculated for silica-gold nanoshells with constant overall size and varying r_1/r_2 (Figure 1c). For nanoshells with $r_2 = 100$ nm, as r_1/r_2 increases from 0.5 to 0.91 the corresponding nanoshell sensitivity increases from 554.7 to 688.6 nm/RIU. An 82% increase in r_1/r_2 increases the SPR sensitivity by only ~19%. Since the plasmon excited in a nanoshell also depends on the interior dielectric,²⁹ the nanoshells with a constant core dielectric are less sensitive to solvent changes than nanoshells in which the core dielectric changes with the solvent. Although SPR sensitivity is enhanced slightly with greater r_1/r_2

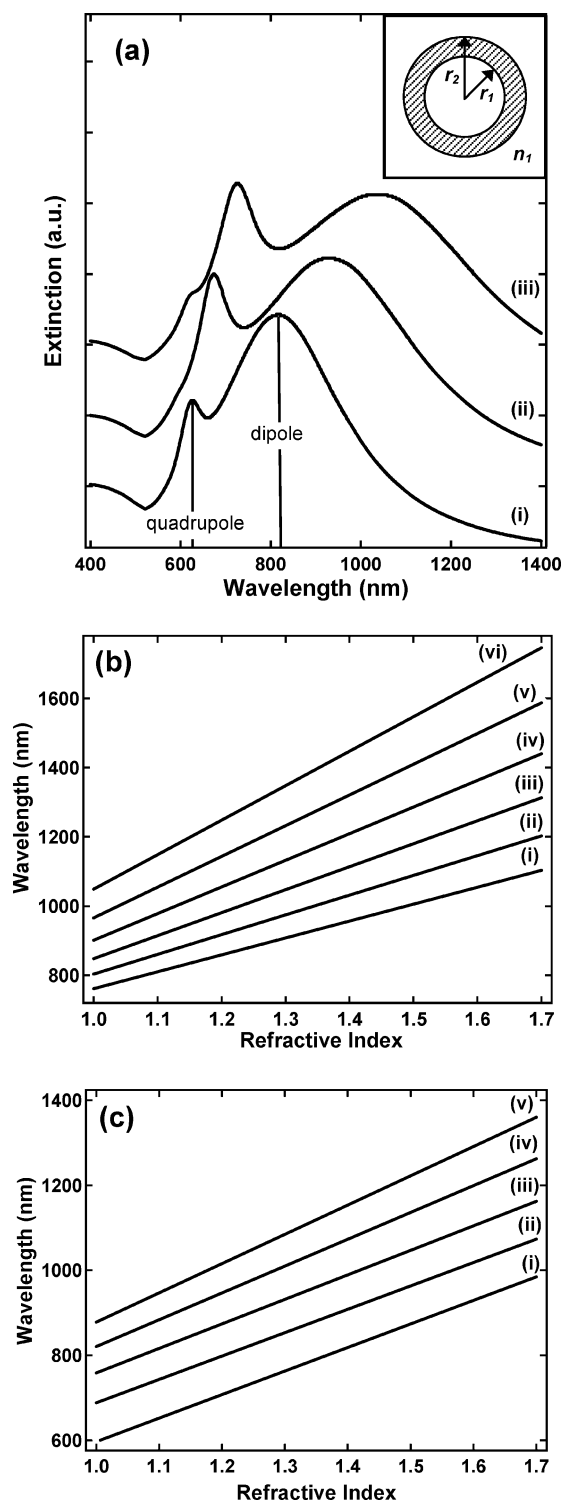


Figure 1. Mie scattering calculations of silica-gold nanoshell extinction. (a) Extinction spectra of a nanoshell with r_1 and $r_2 = 80$ and 100 nm, respectively, in a dielectric environment of refractive index $n_l =$ (i) 1.22 , (ii) 1.45 , and (iii) 1.64 . The peak wavelength of the dipolar resonance of such spectra are plotted as a function of refractive index for nanoshells with (b) a constant r_1/r_2 of 0.9 and $r_2 =$ (i) 50 , (ii) 75 , (iii) 100 , (iv) 125 , (v) 150 , and (vi) 175 nm and (c) nanoshells with $r_2 = 100$ nm and $r_1/r_2 =$ (i) 0.5 , (ii) 0.8 , (iii) 0.86 , (iv) 0.89 , and (v) 0.91 .

r_2 , experimental challenges associated with fabricating very thin gold shells limits the sensitivity enhancement achievable by increasing r_1/r_2 . While these calculations demonstrate that a thinner gold shell is more sensitive to the surrounding dielectric, shell thickness has a less significant effect than increasing the overall particle size for silica-gold nanoshells.

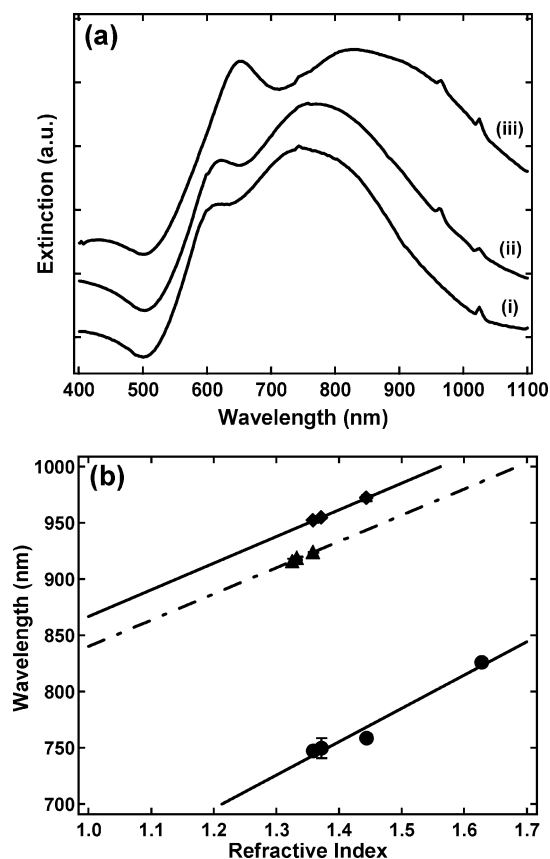


Figure 2. Experimental data from nanoshells suspended in various solvents. (a) Extinction spectra of a nanoshell with r_1 and $r_2 = 60$ and 81 nm, respectively, functionalized with dodecanethiol and suspended in (i) ethanol, $n_l = 1.36$, (ii) chloroform, $n_l = 1.44$, and (iii) carbon disulfide, $n_l = 1.63$. The spectra are offset for clarity. (b) Wavelength peak of the dipole resonance as a function of refractive index for thiolated (solid) and unfunctionalized (dashed) nanoshells. (b) (●) represents the nanoshells r_1 and $r_2 = 60$ and 81 nm, respectively, and (▲, ◆) correspond to nanoshells with r_1 and $r_2 = 60$ and 68 nm, respectively. Error bars that are not visible are smaller than the dimensions of the symbol.

To experimentally verify the trends predicted by Mie scattering calculations, SPR sensitivities were measured for nanoshells in solution (Figure 2a). Figure 2b shows the dipole resonance peak wavelength plotted as a function of refractive index of the surrounding medium. Note that for a nanoshell with r_1 and $r_2 = 60$ and 68 nm, respectively, the addition of dodecanethiol red shifts the dipole resonance 28 nm in ethanol. Changes in the optical spectrum due to dielectric and chemical effects of surface functionalization cannot be modeled exactly using Mie theory.^{8,20} It is common to model an alkanethiol monolayer as a simple thin dielectric layer surrounding a metal, but these models do not accurately predict the optical response of the metal.⁴ Qualitatively, however, the spectra do exhibit the trends predicted by theory. As n_l increases, the resonance peaks red shift and the strength of the quadrupole resonance in comparison to the dipole becomes more significant. Figure 2b shows linear fits to the dipole resonance peak shift as a function of solvent refractive index. Although the quadrupole resonance also red shifts, the dipole resonance is more sensitive to changes in n_l . The larger nanoshells with $r_2 = 81$ nm have a sensitivity of 296.4 nm/RIU as compared to 237 nm/RIU and 233 nm/RIU for the smaller ($r_2 = 68$ nm) nanoshells, despite the fact that the smaller nanoshells have a larger r_1/r_2 . These data support the theoretically predicted conclusion that overall particle size is the dominant parameter controlling SPR sensitivity.

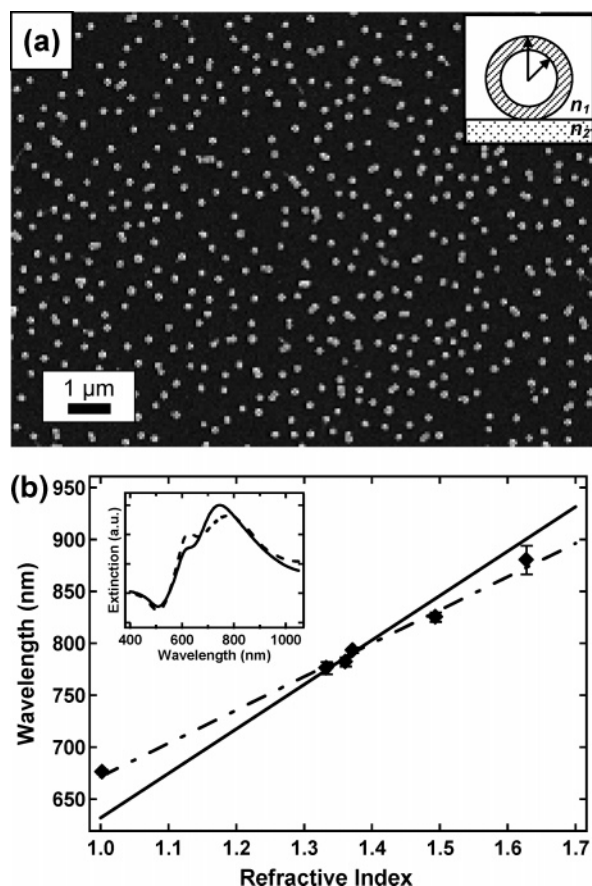


Figure 3. Effect of an inhomogeneous dielectric environment on the optical response of nanoshells. (a) An SEM micrograph of nanoshells deposited onto a glass slide using poly(vinylpyridine). (b) Experimental data (◆, --) of the dipole SPR shift of nanoshells immobilized on a glass slide. The solid lines correspond to theoretical calculations of the nanoshell resonances in a homogeneous medium of corresponding refractive index. Error bars that are not visible are smaller than the dimension of the symbol.

Several studies have investigated the SPR response of nanoparticles on glass surfaces. To compare these results, we also studied the SPR response of nanoshells immobilized on a glass substrate. As the SEM micrograph (Figure 3a) of these nanoshells immobilized on PVP functionalized glass shows, the nanoparticles are well-separated. As a result, these films yield extinction spectra that are characteristic of single nanoparticles with minimal spectral evidence of particle–particle interactions. The films are very robust; exposure of the films to several different organic solvents did not cause spectroscopically detectable particle loss or changes to interparticle spacing.

Since the nanoshells immobilized with PVP are prevented from further aggregation, use of a capping agent such as an alkanethiol is unnecessary. The SPR shifts we observe with these films are more comparable to Mie scattering theory in that the bulk solvent change corresponds to the local dielectric change. However, in a film geometry, the particles are surrounded by an inhomogeneous dielectric environment because they are touching the polymer coated glass on one side. To quantify this effect, we calculated extinction spectra based on the particle dimensions in various solvents and confirmed that the calculated spectrum matched the experimental spectrum in water. The calculated spectra are then compared to experimental spectra of the same nanoshells immobilized on a film and immersed in the solvents. Figure 3b illustrates the difference in sensitivity between nanoshells on a film, 321 nm/RIU, and the calculated sensitivity in solution, 428 nm/RIU. The glass substrate, n_2 ,

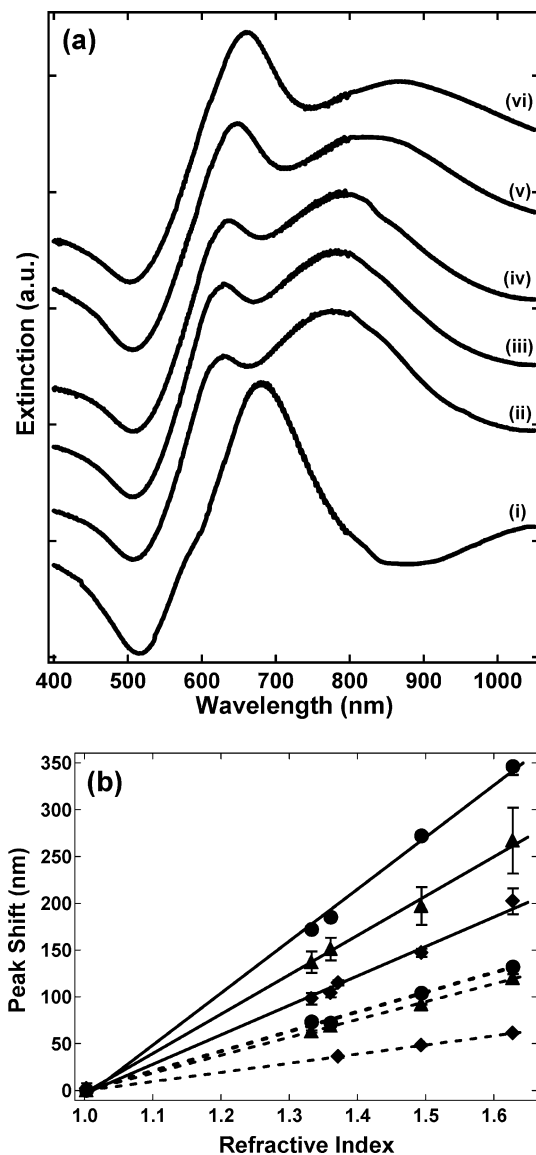


Figure 4. Nanoshell films. (a) Extinction spectra of a nanoshell film with r_1 and $r_2 = 62$ and 81 nm, respectively, immersed in (i) air, $n_1 = 1.003$, (ii) water, $n_1 = 1.33$, (iii) ethanol, $n_1 = 1.36$, (iv) hexane, $n_1 = 1.37$, (v) toluene, $n_1 = 1.49$, and (vi) carbon disulfide, $n_1 = 1.63$. The spectra are offset for clarity. (b) The wavelength of the dipole (solid) and quadrupole (dashed) resonance shifts with respect to air as a function of refractive index for nanoshells with (◆) r_1 and $r_2 = 62$ and 81 nm, respectively, (▲) r_1 and $r_2 = 81$ and 112 nm, respectively, and (●) r_1 and $r_2 = 102$ and 122 nm, respectively. The value for the quadrupole resonance in air is extrapolated from the linear relationship between that exhibited by the data points. Error bars that are not visible are smaller than the dimensions of the symbol.

decreases the sensitivity of the nanoshells to the surrounding dielectric by holding the refractive index of part of each nanoshell's local environment constant. A film of nanoshells on a glass substrate is 25% less sensitive to the solvent dielectric than are nanoshells that are dispersed in the solvent. Nonetheless, the nanoshells function as highly sensitive SPR substrates with sensitivities comparable to and greater than previously reported studies performed with smaller hollow spheres³⁷ (408.8 nm/RIU) and solid silver nanoparticles³⁶ (235 nm/RIU). The evolution of spectral features follows that expected from theory; the resonances red shift, and the quadrupole resonance becomes more significant than the dipole, as shown in Figure 4a.

The dependence of SPR sensitivity on nanoshell geometry is verified with nanoshell films. For nanoshells with $r_2 = 81$,

112, and 122 nm, the SPR sensitivity of the dipole resonance was determined to be 313.9, 420.2, and 555.4 nm/RIU respectively. The largest nanoshells demonstrate the greatest SPR sensitivity. In addition, the largest nanoshells also have a slightly larger r_1/r_2 of 0.836 as compared to 0.765 and 0.723 in the smallest and intermediate sized nanoshells, respectively. This may have also contributed to the increase in sensitivity. However, the lowest r_1/r_2 did not yield the lowest sensitivity, demonstrating that the overall nanoshell size is the dominant sensitivity parameter.

As shown in Figure 4b, the SPR shift of the quadrupole resonance can also be followed as n_l increases. The strengthening of this spectral feature coincides with the spectral broadening of the dipole resonance at high n_l . This means that although broadening makes dipole peak wavelength determination more difficult at higher n_l , the quadrupole peak shift affords another route to monitor changes in n_l . The sensitivity of the quadrupole SPR shift increases with overall particle size, as the dipole resonance does. However, the quadrupole sensitivity is reduced compared to the dipole, with $\Delta\lambda/\Delta n = 97.6$, 190.7, and 210.3 nm/RIU for the small, intermediate, and large nanoshells, respectively. This effect is consistent with Mie Scattering Theory. The ability to follow the quadrupole increases the dynamic range of a nanoshell SPR sensor.

In conclusion, we have proven that we can accurately model the parameters affecting the SPR sensitivity of nanoshells using Mie scattering theory, and that nanoshell SPR sensors can be fabricated with controllable sensitivities. The SPR sensitivity increases dramatically with overall particle size and to a lesser extent with increasing r_1/r_2 . The sensitivity observed is similar to or greater than sensitivities achieved with other metal nanoparticles. SPR sensitivity may be further enhanced by fabricating larger nanoshells with thinner gold shells. Understanding the parameters that control sensitivity offers insight toward the design and engineering of nanoshell sensors for specific SPR applications.

References and Notes

- (1) Kreibitz, U.; Genzel, L. *Surf. Sci.* **1985**, *156*, 678.
- (2) Bohren, C. F.; Huffman, D. R. *Absorption and Scattering of Light by Small Particles*; Wiley: New York, 1983.
- (3) Mulvaney, P.; Liz-Marzan, L. M.; Giersig, M.; Ung, T. *J. Mater. Chem.* **2000**, *10*, 1259.
- (4) Malinsky, M. D.; Kelly, K. L.; Schatz, G. C.; Van Duyne, R. P. *J. Am. Chem. Soc.* **2001**, *123*, 1471.
- (5) Cocchini, F.; Bassani, F.; Bourg, M. *Surf. Sci.* **1985**, *156*, 851.
- (6) Haynes, C. L.; Van Duyne, R. P. *J. Phys. Chem. B* **2003**, *107*, 7426.
- (7) Elghanian, R.; Storhoff, J. J.; Mucic, R. C.; Letsinger, R. L.; Mirkin, C. A. *Science* **1997**, *277*, 1078.
- (8) Mulvaney, P. *Langmuir* **1996**, *12*, 788.
- (9) Jackson, J. B.; Westcott, S. L.; Hirsch, L. R.; West, J. L.; Halas, N. J. *Appl. Phys. Lett.* **2003**, *82*, 257.
- (10) Gunnarsson, L.; Bjerneld, E. J.; Xu, H.; Petronis, S.; Kasemo, B.; Kall, M. *Appl. Phys. Lett.* **2001**, *78*, 802.
- (11) Maier, S. A.; Brongersma, M. L.; Kik, P. G.; Atwater, H. A. *Phys. Rev. B* **2002**, *65*, 193408.
- (12) Weeber, J. C.; Krenn, J. R.; Dereux, A.; Lamprecht, B.; Lacroute, Y.; Goudonnet, J. P. *Phys. Rev. B* **2001**, *64*, 045411.
- (13) Ghaemi, H. F.; Thio, T.; Grupp, D. E.; Ebbesen, T. W.; Lezec, H. J. *Phys. Rev. B* **1998**, *58*, 6779.
- (14) Hirsch, L. R.; Stafford, R. J.; Bankson, J. A.; Sershen, S. R.; Rivera, B.; Price, R. E.; Hazle, J. D.; Halas, N. J.; West, J. L. *Proc. Natl. Acad. Sci. U.S.A.* **2003**, *100*, 13549.
- (15) Loo, C.; Lin, A.; Hirsch, L.; Lee, M. H.; Barton, J.; Halas, N.; West, J.; Drezeck, R. *Technol. Cancer Res. Treat.* **2004**, *3*, 33.
- (16) Homola, J.; Yee, S. S.; Gauglitz, G. *Sens. Actuators, B* **1999**, *54*, 3.
- (17) Nelson, B. P.; Frutos, A. G.; Brockman, J. M.; Corn, R. M. *Anal. Chem.* **1999**, *71*, 3928.
- (18) Lofas, S.; Malmqvist, M.; Ronnberg, I.; Stenberg, E.; Liedberg, B.; Lundstrom, I. *Sens. Actuators, B* **1991**, *5*, 79.
- (19) Haes, A. J.; Van Duyne, R. P. *J. Am. Chem. Soc.* **2002**, *124*, 10596.
- (20) Templeton, A. C.; Pietron, J. J.; Murray, R. W.; Mulvaney, P. *J. Phys. Chem. B* **2000**, *104*, 564.
- (21) Kreibitz, U.; Vollmer, M. *Optical Properties of Metal Clusters*; Springer-Verlag: Berlin, 1995.
- (22) Hirsch, L. R.; Jackson, J. B.; Lee, A.; Halas, N. J.; West, J. *Anal. Chem.* **2003**, *75*, 2377.
- (23) Kneipp, K.; Wang, Y.; Kneipp, H.; Itzkan, I.; Dasari, R. R.; Feld, M. S. *Phys. Rev. Lett.* **1996**, *76*, 2444.
- (24) Nie, S. M.; Emery, S. R. *Science* **1997**, *275*, 1102.
- (25) Moskovits, M. *Rev. Mod. Phys.* **1985**, *57*, 783.
- (26) Oldenburg, S. J.; Averitt, R. D.; Westcott, S. L.; Halas, N. J. *Chem. Phys. Lett.* **1998**, *288*, 243.
- (27) Averitt, R. D.; Sarkar, D.; Halas, N. J. *Phys. Rev. Lett.* **1997**, *78*, 4217.
- (28) Prodan, E.; Radloff, C.; Halas, N. J.; Nordlander, P. *Science* **2003**, *302*, 419.
- (29) Prodan, E.; Lee, A.; Nordlander, P. *Chem. Phys. Lett.* **2002**, *360*, 325.
- (30) Oldenburg, S. J.; Hale, G. D.; Jackson, J. B.; Halas, N. J. *Appl. Phys. Lett.* **1999**, *75*, 1063.
- (31) Westcott, S. L.; Jackson, J. B.; Radloff, C.; Halas, N. J. *Phys. Rev. B* **2002**, *66*, 155431.
- (32) Malynych, S.; Luzinov, I.; Chumanov, G. *J. Phys. Chem. B* **2002**, *106*, 1280.
- (33) Duff, D. G.; Baiker, A.; Edwards, P. P. *Langmuir* **1993**, *9*, 2301.
- (34) Mie, G. *Ann. Phys.* **1908**, *24*, 377.
- (35) Jensen, T. R.; Duval, M. L.; Kelly, K. L.; Lazarides, A. A.; Schatz, G. C.; Van Duyne, R. P. *J. Phys. Chem. B* **1999**, *103*, 9846.
- (36) McFarland, A. D.; Van Duyne, R. P. *Nano Lett.* **2003**, *3*, 1057.
- (37) Sun, Y. G.; Xia, Y. N. *Anal. Chem.* **2002**, *74*, 5297.